Optical Engineering

SPIEDigitalLibrary.org/oe

Design and analysis of an alignment procedure using computer-generated holograms

Laura E. Coyle
Matthew B. Dubin
James H. Burge

SPIE

Design and analysis of an alignment procedure using computer-generated holograms

Laura E. Coyle
Matthew B. Dubin
James H. Burge
University of Arizona
College of Optical Sciences
1630 East University Boulevard
Tucson, Arizona 85721
E-mail: lcoyle@optics.arizona.edu

Abstract. A procedure that uses computer-generated holograms (CGHs) to align an optical system's meters in length with low uncertainty and real-time feedback is presented. The CGHs create simultaneous three-dimensional optical references, which are decoupled from the surfaces of the optics allowing efficient and accurate alignment even for systems that are not well corrected. The CGHs are Fresnel zone plates, where the zero-order reflection sets tilt and the first-diffracted order sets centration. The flexibility of the CGH design can be used to accommodate a wide variety of optical systems and to maximize the sensitivity to misalignments. An error analysis is performed to identify the main sources of uncertainty in the alignment of the CGHs and to calculate the magnitudes in terms of general parameters, so that the total uncertainty for any specific system may be estimated. A system consisting of two CGHs spaced 1 m apart is aligned multiple times and re-measured with an independent test to quantify the alignment uncertainty of the procedure. The calculated and measured alignment uncertainties are consistent with less than 3 μrad of tilt uncertainty and 1.5 μm of centration uncertainty (1σ). [DOI: 10.1117/1.OE.52.8.084104]

Subject terms: optical alignment; alignment datum; computer-generated holograms; Fresnel zone plates.

Paper 130696P received May 10, 2013; revised manuscript received Jul. 23, 2013; accepted for publication Jul. 24, 2013; published online Aug. 28, 2013.

1 Introduction

As the technologies for manufacture and metrology advance, optical systems are being designed with more complexity than ever before. Given these prescriptions, alignment can be a limiting factor in determining their final performance. Systems for astronomical telescopes, lithography, and high-energy lasers may require the alignment of multiple components with micron-level accuracy over many meters. The goal of this work is to develop a low-uncertainty alignment procedure that can be applied to a variety of optical systems.

There are many tools, mechanical and optical, available for alignment. A coordinate measuring machine (CMM) uses a touch probe to measure the position of features in three dimensions. With careful operation, a CMM can obtain a repeatability of 3 μm along a single-measurement axis with an additional uncertainty of 3 μm/m over large volumes.[1] However, a CMM is not practical for large assemblies, as the largest CMMs are only a few meters in length; also, the optics are commonly housed in mechanical structures that restrict the probe's access to datum features. CMMs cannot provide real-time feedback of the system alignment and make the process lengthy. Laser trackers are also used for optical alignment.[2] They have a typical accuracy of $4\,\mu\text{m} \pm 0.8\,\mu\text{m/m}$.[3] Operation requires a line of sight from the tracker to a sphere-mounted retro-reflector target in contact with a datum, which also can be hindered by the mechanical mounting structure. Real-time feedback of the system alignment can only be obtained with multiple measurements, and thus, multiple laser trackers are required, which is often prohibitively expensive. Alignment telescopes and axicons create an optical axis that can be used to center components. The centration accuracy depends on the straightness of the axis and the ability to align targets to it.[4–6] In a previous experiment, an alignment telescope with camera eyepiece was rotated on an air bearing to maximize alignment precision, but the centration uncertainty for a target at a distance of 1 m was 15 μm 1σ.[7] For both methods, an additional test is needed to measure the tilt.

This procedure uses computer-generated holograms (CGHs) to create simultaneous three-dimensional optical references and to perform an alignment in multiple degrees of freedom with real-time feedback. The optical references are decoupled from the surfaces of the optics allowing accurate alignment even for systems that are not well corrected. Transferring the alignment datum to an external reference, this procedure describes the alignment of CGHs, which must be separately aligned to the optics. The sensitivity of the instruments used to track the optical references is a driving factor in the final uncertainty; yet good performance can be achieved with off-the-shelf components. This procedure is designed to achieve centration uncertainties of a few microns and tilt uncertainties of a few micro-radians over a distance of several meters.

In this article, we describe how to use CGHs to align an optical system and to quantify the residual uncertainty. Section 2 outlines the procedure and describes the advantages of using CGHs to create the optical references. The major sources of uncertainty are identified in Sec. 3, and their magnitudes are calculated in terms of general parameters, so that the total uncertainty for any specific system may be estimated. Finally, Sec. 4 presents experimental results for the alignment uncertainty a two CGH system and compares it with the expected uncertainty from the analysis in Sec. 3.

2 CGH Alignment Procedure

The goal of this procedure is to align axi-symmetric aspheric optics in four degrees of freedom, two each in tilt and in centration. Rather than using the optical surfaces, the alignment data is transferred to an external reference—a CGH—written to an optical flat with a reference mark at the pattern's center. The CGH is rigidly mounted to the optic such that the CGH surface normal represents the tilt of the optic, and the reference mark represents the optical axis. If the CGH is accurately aligned to the optical surface, well-aligned CGHs will produce a well-aligned system. The ideal alignment case requires the reference mark at the center of each CGH pattern be coincident with a single axis and the surface normal of the CGH be parallel to that axis.

The alignment procedure uses CGHs that are written with Fresnel zone plate (FZP) patterns, so they act like thin lenses. One CGH (CGHA) creates two focused spots, which define the alignment axis, and then a second CGH (CGHB) is aligned to that axis. The CGHs are aligned in centration pairwise using a single CGHA, so the alignment axis is maintained, and multiple CGHBs with different patterns for a system with three or more optics. The label CGHB is used for optics 2 through n since the alignment procedure and error analysis equations are the same for these CGHs. Any single CGHB is aligned to CGHA with all the others removed. An autocollimator is used to align the tilt of each CGH independently.

2.1 *Computer-Generated Holograms*

CGHs with varying degrees of complexity have been used to perform alignment of optical components, often by using the optical surfaces.[8,9] The CGHs in this procedure are decoupled from the optics and are designed simply to act like lenses, though they are preferable to lenses for two main reasons. First, the CGH patterns are created using a laser writer for photomasks, and a center reference mark is written with submicron precision. It is difficult to measure the center of a lens to the same accuracy. Second, multiple patterns can be combined on a substrate, so a single CGH can act like two lenses with the same axis, but different focal lengths.

Our CGHs use two types of patterns. CGHA consists of two concentric FZPs with different focal lengths, and CGHB contains only one FZP. While the axial spacing of the CGHs is likely constrained by the optical and mechanical designs, the focal lengths of the FZPs are degrees of freedom. These focal lengths can be chosen to increase the sensitivity to centration error.

The CGHs can be phase etched, chrome-on-glass, or a combination. Their design allows flexibility for the intensity in each diffracted order. The desired intensity is in the zero and first orders specifically, and the wavelength range of the source must be considered when choosing the etch depth or duty cycle of the CGHs. The non-CGH side of the substrate is anti-reflection coated to avoid unwanted ghosts.

2.2 *Alignment of CGHs to Optical Surfaces*

This article describes the alignment of CGHs, which must also be individually aligned to an optical surface to achieve the desired system performance. For an aspheric mirror, there is a single optical axis. The CGHs must be aligned to the optic such that the center of the CGH pattern is coincident with the mirror's optical axis, and its surface normal is parallel to the mirror's axis, as in Fig. 1. Since this procedure is not meant to set the axial spacing, the CGH center mark need not be coincident with the mirror's vertex.

To align the CGH to the optic, the optic is mounted on a rotary bearing. Its tilt and centration are adjusted until the optical axis is coincident with the bearing's mechanical axis. This can be done by placing the optic under an interferometric test and by minimizing the change in the measurement as the part rotates. Then, the CGH is mounted in the center of the optic and independently positioned to minimize lateral and angular runout. Once both the optic and CGH are aligned to the bearing axis, they are aligned to each other, and the CGH is fixed in place. This alignment can be performed to submicron accuracy, limited only by the quality of the bearing and the precision of the mechanics and diagnostics.

The error analysis in Sec. 3 applies to the CGHs only. Error analysis for the optical surfaces, as a result of misalignment between the CGH and optic, is outside the scope of this paper. Once the system is aligned, an additional test using the optical surfaces can be used to quantify the effect of the CGH-optic misalignment on the system performance.

This procedure is well suited for aligning axi-symmetric optics with central holes. For off-axis systems or those without central holes, a set of CGHs can be mounted at the edge of the optics and aligned; but a second set of CGHs is needed to control clocking of the optics about the axis of the first set.

2.3 *Alignment Procedure*

Once the CGHs are individually aligned to the optics, the CGHs are aligned in centration and tilt. For the ideal alignment, the center mark of each CGH is coincident with a single axis, and the surface normals are parallel to that axis.

Since the CGHs are written onto plane parallel plate substrates, an autocollimator is a convenient reference to set the tilt. The autocollimator measures the angle between the zero order or the specular reflection from the CGH surface and the incident beam. The angle of the CGH (or the autocollimator) is adjusted until the incident and reflected beams are parallel, meaning the beam is normally incident on the CGH surface. The autocollimator beam provides an external datum for tilt,

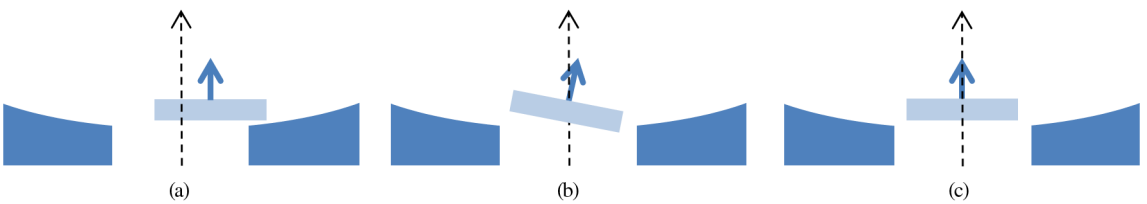

Fig. 1 A rotary bearing is used to align the computer-generated hologram (CGH) to the optical surface. (a) The CGH is aligned in tilt only. (b) The CGH is aligned in centration only. (c) The CGH is aligned in tilt and centration.

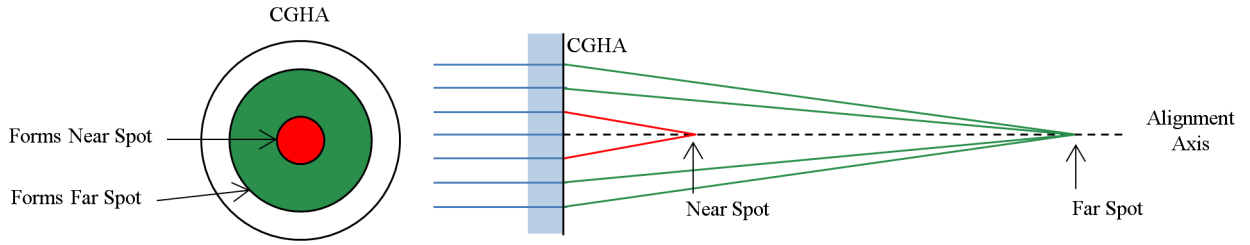

Fig. 2 CGHA has concentric inner and outer regions that create the near spot and the far spot, respectively. The outer CGH is an annulus and does not overlap the inner CGH.

and the CGHs are aligned individually with all the others removed, so a misalignment of one CGH will not propagate. To avoid disturbing the alignment when one is removed, the CGHs must be mounted using stable kinematic interfaces.

Once the CGHs are aligned in tilt, they are aligned pairwise in centration. Section 2.1 described a two zone CGHA that creates two focal points called the "near spot" and "far spot." The CGHA pattern and the axial layout are shown in Fig. 2.

CGHA is illuminated with the same autocollimator beam, approximately centered on the CGH pattern. The alignment axis is defined by the near and the far spots, but it also passes through the center of the CGH pattern because the FZPs are concentric. This holds even if the autocollimator beam is not normally incident on the CGH. Thus, using CGHA to define the alignment axis means it cannot be decentered. This assumes that the autocollimator beam has a well-corrected wave front, since asymmetric aberrations like coma will introduce different amounts of tilt across the inner and outer zones and cause centration error, as discussed in Sec. 3.2.

CGHB is inserted between the near and the far spots, and its $+1$ order images the near spot onto the plane of the far spot. When CGHB is decentered, the image of the near spot is displaced from the far spot, as in Fig. 3. CGHB is adjusted until the image of the near spot coincident with the far spot, meaning CGHB is centered on the alignment axis.

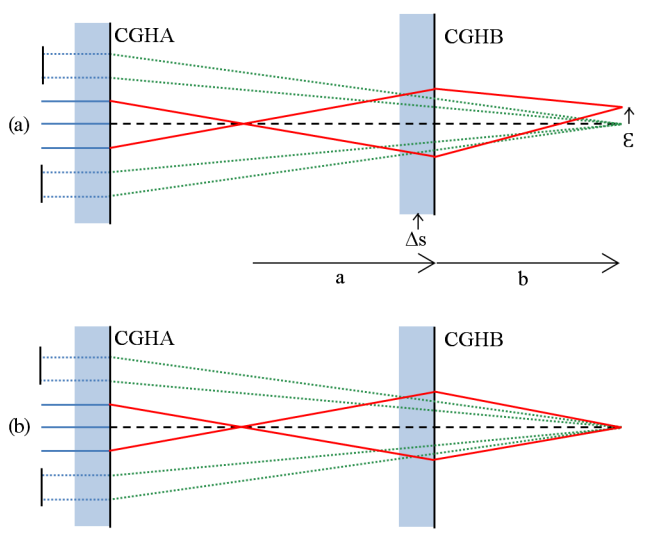

Fig. 3 The $+1$ order of CGHB images the near spot onto the plane of the far spot to perform the centration alignment. (a) The spots are displaced by ε when CGHB is decentered by Δs. (b) The two spots are coincident for a centered CGHB. The rays from the outer zone of CGHA, which form the far spot, are blocked in this step (see Fig. 4), but are shown here for reference.

The relationship between CGHB misalignment (Δs) and the spot misalignment (ε) in terms of distances in Fig. 3 is given by

$$\varepsilon = \Delta s\left(\frac{a+b}{a}\right) = \Delta s(1-m), \tag{1}$$

where m is the magnification of CGHB. The generalized relationship between motion of an optic and the resulting image motion is provided by Burge.[10] The sensitivity to misalignments can be increased by choosing FZP patterns such that $b/a > 1$. If multiple CGHBs are needed, they will have different sensitivities which decrease with distance from CGHA (the distance $a + b$ is fixed by the design of CGHA). As a result, CGHA should be placed at the end of the optical system with the tightest centration requirements. In addition, if there is a constraint on the position of the alignment axis with respect to some other feature, CGHA can be positioned accordingly.

Note that the same beam is used to define the alignment datum for tilt and centration. This choice produces lower uncertainty than two separate data, which would have to be aligned very precisely in angle.

This procedure is not meant to set the axial spacing of the CGHs. Errors in the axial spacing will not affect the tilt alignment, but will cause the far spot and the re-imaged near spot to be out-of-focus in the ideal far spot plane. Small amounts of defocus will still yield circular spots that can be accurately centroided. The amount of allowable axial misalignment will depend on the system geometry, but is on the order of millimeters for slow systems.

Two instruments are required to perform the alignment. The first is an autocollimator, which sets the tilt alignment and creates the alignment axis for centration. The second is a focal plane, where the separation between the far spot and the re-imaged near spot is measured for the centration alignment.

A custom autocollimator was built from off-the-shelf parts with two specific features.[11] First, a narrow line width source was used to minimize the chromatic effects from the CGHs. Second, an iris was added to adjust the output beam diameter. As shown in Fig. 2, the FZP that creates the far spot is an annulus surrounding the FZP that creates the near spot. Once the location of the far spot centroid is recorded in the focal plane, the beam can be stopped down, creating the near spot only. This is helpful for centering CGHB (see Fig. 3), since it is easier to align a single centroid to a known position than to measure the distance between the centroids of overlapping spots.

The autocollimator must be calibrated to find the reference angle for a correctly aligned CGH, where the surface

normal is parallel to the alignment axis/autocollimator beam. To set this reference, a corner cube is used to retroreflect the outgoing beam, which simulates a normal reflection from a surface, and the centroid of the focused return beam is recorded in the autocollimator focal plane. This calibration requires a high-quality corner cube that is well centered on the beam.

The centration error of CGHB is measured in the focal plane with a bare detector or an optical system with magnification to increase the sensitivity. The accuracy of the centration alignment depends on the resolution of the focal plane, the magnification of the optical system, the size/quality of the spots being centroided, and the CGH mechanics. To maximize sensitivity, an optical system was built from an infinity-corrected microscope objective and tube lens to obtain a favorable magnification with a CCD camera at the re-imaged focal plane.[11]

The focal plane measures relative displacements, so the test does not rely on accurate calibration. Any error in the knowledge of the magnification becomes negligible when the spots overlap. The focal plane should be aligned, so the sensor is nominally perpendicular to the alignment axis, and both spots are centered in the field of view to minimize aberrations. Small amounts of sensor's defocus will not affect the centroid location as long as the autocollimator beam wave front is well corrected.

The step-by-step procedure to align the CGHs is shown in Fig. 4.

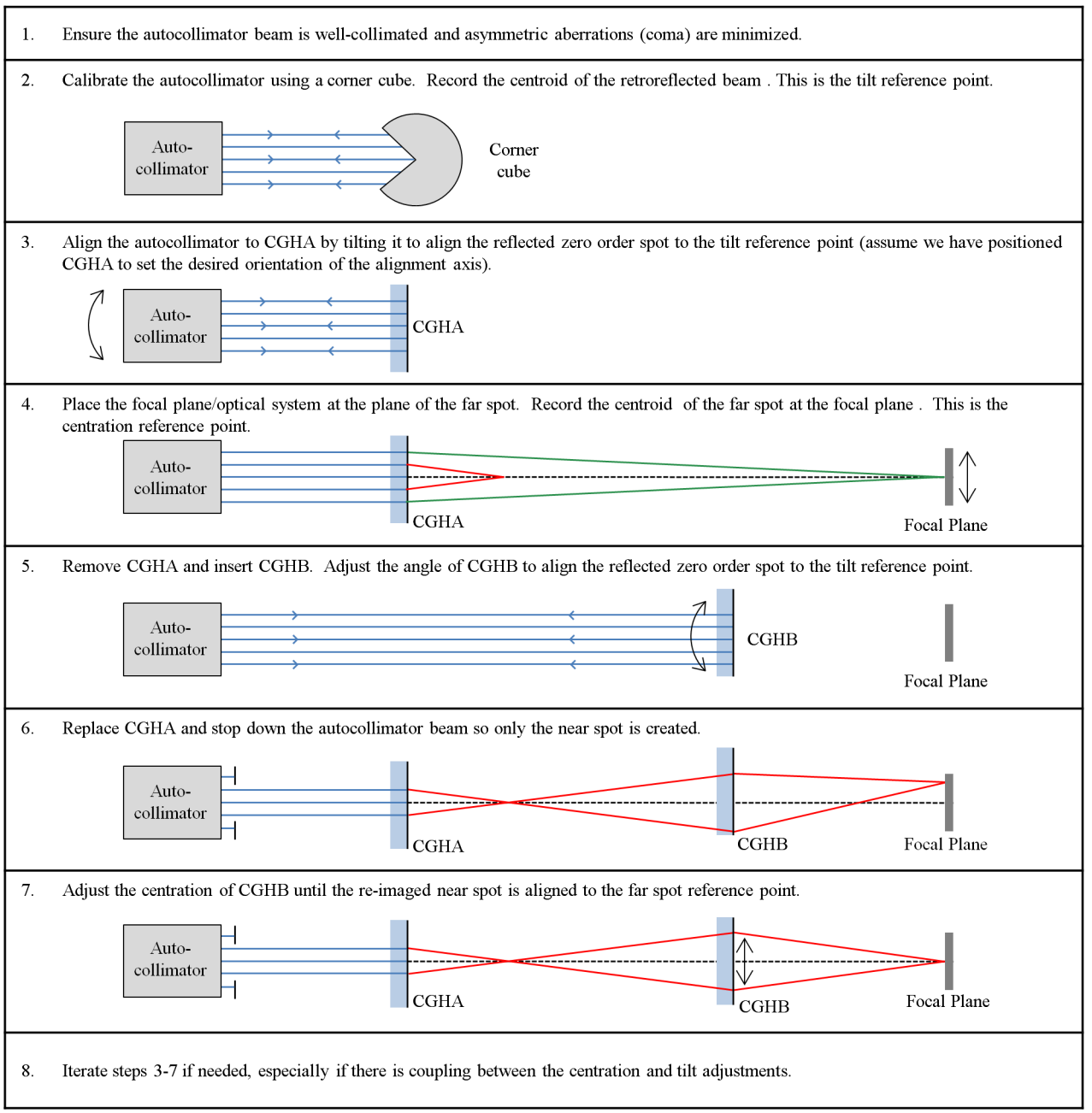

Fig. 4 The step-by-step procedure to align the CGHs in tilt and centration. For a system with three or more optics, after aligning the two CGHs, remove the first CGHB and repeat steps 5–7 to align additional CGHBs. These CGHBs which will have different axial positions and FZP focal lengths so the near spot is re-imaged to the same far spot plane.

3 Error Analysis

The accuracy of the procedure depends on systematic errors in the components and random errors from noise. Analysis is provided for the following error sources:

- Autocollimator calibration
- Autocollimator beam wave front
- Spot centroiding
- Resolution of alignment hardware
- Repeatability of kinematic mounts
- Wedge in CGH substrates
- Writing error for CGH patterns
- Atmospheric effects
- Temperature effects.

3.1 *Autocollimator Calibration*

The autocollimator is calibrated using a corner cube to simulate the reflection from a CGH aligned in tilt. Errors in the corner cube and beam wave front will bias the calibration and create systematic alignment errors.

Real corner cubes often have a specified maximum angular error for a beam exiting in any of its six subapertures. When the beam is centered on the corner cube vertex, the error from each subaperture cancels. For an offset beam, the errors will not cancel. The total angular error for a decentered beam was calculated by weighting the sum of the vector angular error from each subaperture by the illuminated area. Figure 5 shows the angular error in the reflected beam normalized to the maximum single subaperture error for small decenters.

The angular error in the corner cube calibration is given by

$$\text{Tilt Error}(\text{CGHA}, \text{CGHB}) = \frac{\alpha(x) \times E}{2}, \tag{2}$$

where $\alpha(x)$ is the normalized angular error as a function of the beam diameter and offset (see Fig. 5) and E is the

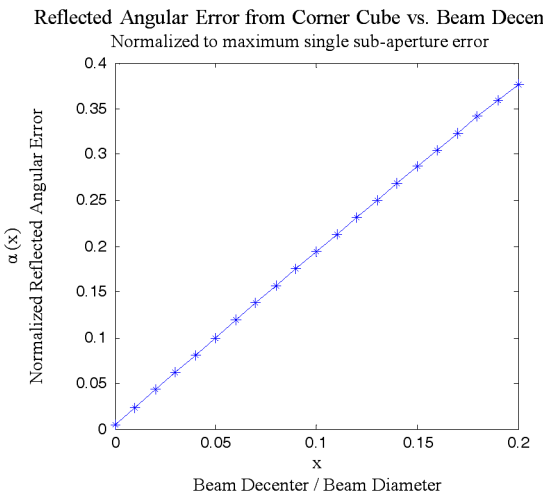

Fig. 5 Plot of normalized angular error from a corner cube as a function of beam diameter and offset.

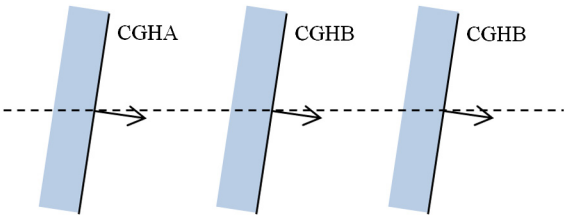

Fig. 6 Error in the corner cube calibration will cause a correlated tilt error in all CGHs.

maximum reflected error from a single subaperture. Since the same calibration is used for all CGHs, the tilt error is correlated, as in Fig. 6. The CGH surface normals are parallel to each other, but not to the alignment axis.

The surface normal of CGHA can be chosen as the angular datum rather than the beam direction. Tilt errors become CGHB centration errors, which is given by

$$\text{Centration Error}(\text{CGHB}) = \left(\frac{\alpha(x) \times E}{2}\right) d + t \frac{\alpha(x) \times E}{2} \left(\frac{n-1}{n}\right), \tag{3}$$

where d is the distance between CGHA and CGHB, t is the substrate thickness, and n is the substrate index of refraction. The second term is a correction, due to the fact that the CGHs have some thickness; but for thin substrates (<10 mm) and small beam angles (<10 μrad), it is negligible.

3.2 *Autocollimator Beam Wavefront*

Equations (2) and (3) must be modified if there are aberrations in the autocolllimator beam. The calibration described in Sec. 2.3 records the centroid of the focused return beam, which will shift in the presence of asymmetric aberrations like coma. The centroid shift, and the corresponding reflected angular error (θ), may be complex but can be simulated in ray tracing code. The new tilt and centration errors are given by

$$\text{Tilt Error}(\text{CGHA}, \text{CGHB}) = \frac{\alpha(x) \times E + \theta}{2} \tag{4}$$

$$\text{Centration Error}(\text{CGHB}) = \left[\frac{\alpha(x) \times E + \theta}{2}\right] d + t \frac{\alpha(x) \times E}{2} \left(\frac{n-1}{n}\right), \tag{5}$$

where $\alpha(x)$ is the normalized angular error, E is the maximum reflected error from a single subaperture, θ is the additional reflected angular error from the centroid shift due to aberrations in the beam, d is the distance between CGHA and CGHB, t is the substrate thickness, and n is the substrate index of refraction. Only one of the above equations is used in the error calculation, which depends on the chosen angular datum.

Asymmetric aberrations will also cause different amounts of tilt across the inner and outer zones of CGHA. Figure 7

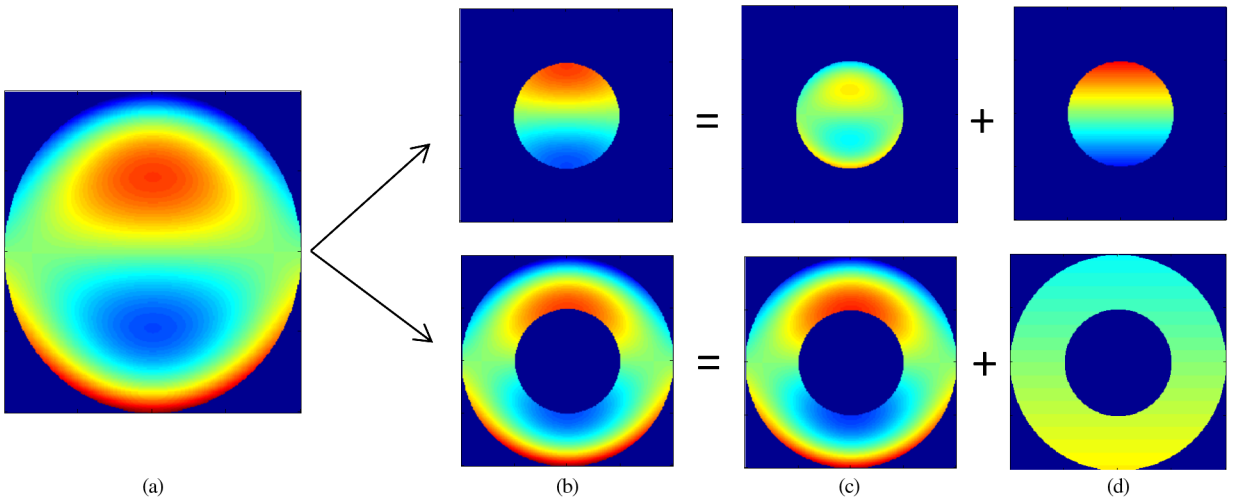

Fig. 7 (a) The beam wavefront contains 1-wave RMS of coma. (b) The wavefront is split into the inner and outer zones of CGHA. Each zone wavefront can be expressed as the sum of (c) some aberration and (*d*) the mean tilt. The mean tilt in each zone will cause angular deviation of the wavefront.

shows the mean tilt across each zone when there is coma in the wave front.

The mean tilt can be converted to the angle of the exiting wave front with respect to the alignment axis using the following equations:

$$\alpha = \frac{T_i \lambda}{D_i} \tag{6}$$

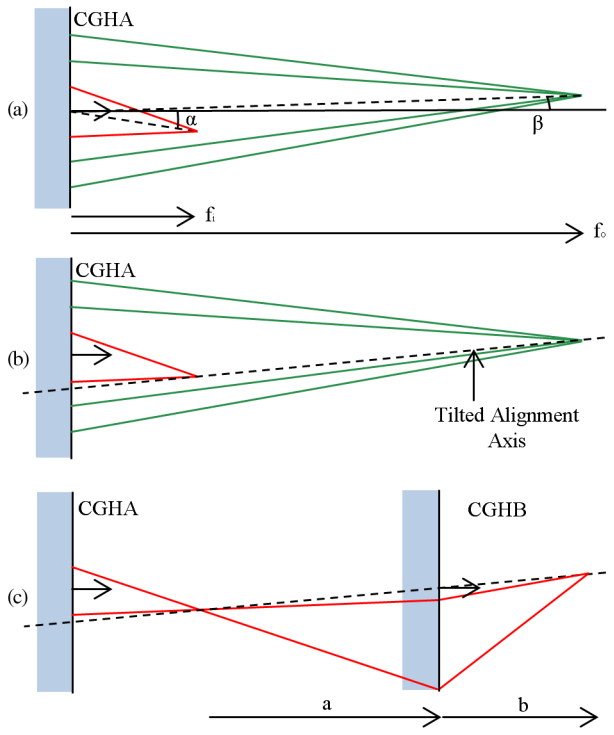

Fig. 8 (a) Coma in the autocollimator beam will cause a tilt α in the beam that creates the near spot and a tilt β in the beam that creates the far spot. (b) The displaced near and far spots create a tilted alignment axis. CGHA has tilt and centration errors. (c) CGHB has only tilt error.

$$\beta = \frac{T_o \lambda}{D_o}, \tag{7}$$

where α is the wavefront angle of the inner zone, β is the wave front angle of the outer zone, D_i and D_o are the diameters of the inner and outer zones, respectively, T_i and T_o are the peak-to-valley mean tilts in waves across the inner and outer zones, respectively, and λ is the wavelength. Figure 8 illustrates how tilt differences between the zones cause alignment error for both CGHA and CGHB.

The tilt and centration errors in CGHA are given by

$$\text{Tilt Error(CGHA)} = \frac{\beta f_o - \alpha f_i}{f_o - f_i} \tag{8}$$

$$\text{Centration Error(CGHA)} = f_i \left(\frac{\beta f_o - \alpha f_i}{f_o - f_i} - \alpha \right), \tag{9}$$

where f_i and f_o are the focal lengths of the inner and outer FZPs, respectively, α is the wave front angle of the inner zone, and β is the wave front angle of the outer zone.

CGHB will have the same tilt error as CGHA [Eq. (8)], but no centration error with respect to the tilted alignment axis. If other aberrations cause wave front tilt in the orthogonal direction, the tilt and centration errors in each direction are calculated using the previous equations, and the results are root sum squared.

3.3 *Spot Centroiding*

The tilt reference from the autocollimator calibration and the far spot centration reference are set by centroiding spots on electronic detectors. There will be random errors in the measured centroid location due to the detector noise, vibrations, air currents, spot quality, and other sources. The location of the optical references that need to be aligned to these reference points will have similar errors. The magnitude of the spot centroiding uncertainty must be estimated for the specific hardware and environment and take both spots into account.

3.4 *Resolution of Alignment Hardware*

The ability to align the optical references to the calibrated points will be limited by the CGH alignment hardware. Resolution, adjustment coupling, and other sources will limit the ability to perfectly align the spots to the desired locations.

3.5 *Repeatability of Kinematic Mounts*

As shown in Fig. 4, CGHA is removed after the far spot reference is recorded, so CGHB can be aligned in tilt. If the mounts are not repeatable, the far spot reference from the replaced CGHA will be different from its original marked location, and an "aligned" CGHB will be decentered. The decenter of CGHB is calculated using Eq. (1), where ε is the change in the far spot location after replacing CGHA.

3.6 *Wedge in Substrates*

Thus far, our analysis has assumed that the substrates are ideal plane parallel plates. Real substrates will have some wedge adding both tilt and centration errors.

3.6.1 *Wedge in CGHA*

Wedge in CGHA is completely accommodated if the CGH surface is the datum for the alignment. As shown in Fig. 9, the autocollimator is tilted to align CGHA in angle and, by definition, CGHA cannot be decentered. However, the autocollimator beam is not parallel to the alignment axis when CGHA is removed, which couples into the alignment errors for CGHB.

3.6.2 *Wedge in CGHB*

When CGHA is removed to align CGHB in tilt (assume same orientation of alignment axis), the angle of the autocollimator beam and the wedge in CGHB will cause an aligned CGHB to appear to have a tilt error, as in Fig. 10.

The wedge in CGHB can be split into two orthogonal components (α_{B1} and α_{B2}), one of which is aligned to the wedge in CGHA (α_A). For the component aligned to the CGHA wedge (α_{B1}), the tilt error is

$$\text{Tilt Error1(CGHB)} = \alpha_{B1}(n-1) - \alpha_A(n-1), \tag{10}$$

where n is the index of refraction for the substrates and the sign of the substrate wedge must be consistent. For

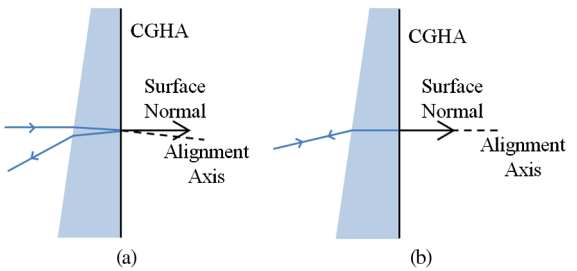

Fig. 9 CGHA is written to a substrate with wedge. (a) When the autocollimator beam is parallel to the CGH surface normal, the CGH is misaligned. (b) The autocollimator is tilted until the beam is normally incident on the CGH. The surface normal and alignment axis are parallel as desired.

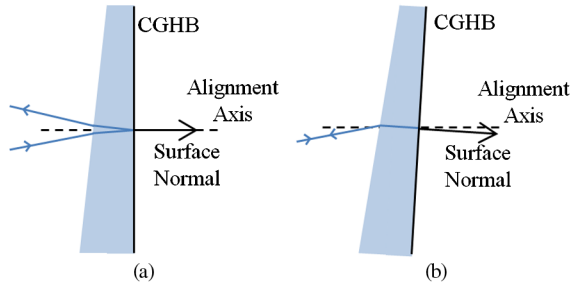

Fig. 10 The tilted autocollimator beam is incident on CGHB. (a) When the CGHB surface normal is parallel to the alignment axis, it appears misaligned. (b) CGHB is tilted to retroreflect the beam adding tilt error.

the component perpendicular to the CGHA wedge (α_{B2}), the only source of tilt error is wedge in CGHB.

$$\text{Tilt Error2(CGHB)} = \alpha_{B2}(n-1). \tag{11}$$

The total tilt error for CGHB is the root sum square of the two orthogonal contributions.

CGHB wedge will also cause centration error, as in Fig. 11. The magnitude of this error is given by

$$\text{Centration Error(CGHB)} = -\frac{\alpha_B(n-1)d}{(1-m)}, \tag{12}$$

where α_B is the total wedge in CGHB, d is the distance between CGHB and the far spot, and m is the magnification of the CGHB FZP.

In practice, all substrates have some wedge. Wedge in CGHA will cause a correlated error in all CGHBs, so it is worthwhile to choose that particular substrate to have the lowest wedge. The effects can be calibrated by biasing the alignment if the wedge magnitude and orientation in each substrate is known. It can be avoided altogether if CGHB is aligned in tilt with CGHA present. However, it is more difficult to centroid overlapping spots, potentially increasing the error described in Sec. 3.3.

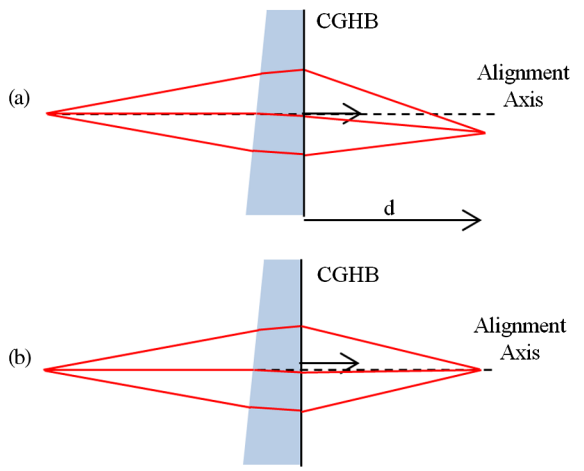

Fig. 11 CGHB re-images the near spot onto the plane of the far spot. (a) A centered CGHB with wedge will create a displacement between the spots. (b) CGHB is decentered to align the spots.

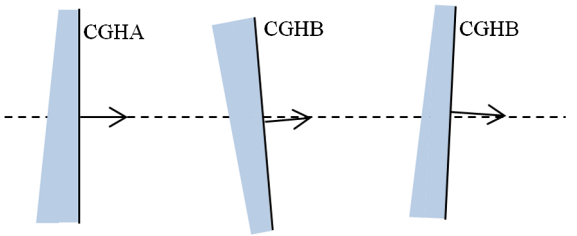

Fig. 12 The CGHs are written to the rear surface of a substrate with wedge. The arrows represent the center and the tilt of the CGH illustrating the possible alignment errors due to wedge.

3.6.3 *Substrate wedge and CGH orientation*

The previous analysis has assumed that the CGHs are written to the rear side of substrates with wedge, which will produce errors that look like Fig. 12 (consider errors only from wedge).

The substrates could be flipped, so the CGHs are on the front of the substrates producing a different set of alignment errors. CGHA is still the alignment datum and has no tilt or centration error. However, the alignment axis is refracted by the wedged substrate causing centration error for CGHB. There is an additional centration error from CGHB wedge. All the substrates will be parallel, unlike the previous case, but will be tilted with respect to the alignment axis. A possible alignment for this case is shown in Fig. 13.

Depending on the system in question and the requirements on centration and tilt, one must decide whether the alignment in Figs. 12 or 13 is preferable.

3.7 *Writing Error*

By definition, CGHA cannot be decentered because the FZP patterns are concentric. If the patterns are not concentric due to writing error, the alignment axis does not pass through the center of CGHA nor is it perpendicular to the CGHA or CGHB surface normals. This will cause tilt and centration error for both CGHs, similar to the analysis in Sec. 3.2. CGHB could have additional alignment error if the writing error added a tilt carrier to either CGH. Measurements of actual CGHs have yielded position errors of 10 to 15 nm 1σ[12] producing negligible alignment error for most of the systems.

3.8 *Atmospheric Effects*

In a stable environment, air layering and temperature gradients can cause a GRIN effect refracting the autocollimator beam as it propagates.[13] Integrating the angular deviation of the beam over the path L gives the total displacement (CGH centration error)

$$\text{Centration Error}(\text{CGHA}, \text{CGHB}) = x = \int_0^L \frac{\Delta n(z)}{w(z)}(L - z)\mathrm{d}z, \tag{13}$$

where $w(z)$ is the beam diameter and $\Delta n(z)/w(z)$ is the change in index across the beam, and both are a function of axial position (z). The tilt error is given by the slope of the displacement curve at the CGH

$$\text{Tilt Error}(\text{CGHA}, \text{CGHB}) = \left.\frac{\partial x}{\partial z}\right|_{z=L}. \tag{14}$$

This effect will only add significant error for systems with long air paths in a stagnant environment. To get a 1-μm centration error for a system with a 1-m air path, the change in temperature across the beam diameter must exceed 2°C ($\mathrm{d}n/\mathrm{d}T = 1e-6/°\mathrm{C}$).

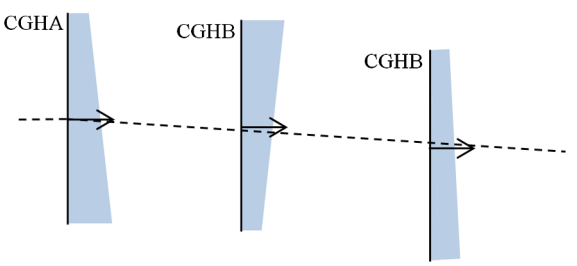

Fig. 13 The CGHs are written to the front surface of a substrate with wedge. The arrows represent the center and the tilt of the CGH illustrating the possible alignment errors due to wedge.

3.9 *Thermal Effects*

Temperature gradients also affect the substrates, alter the index of refraction, and create a thermal wedge. This wedge can be calculated from the coefficient of thermal expansion for the substrate (CTE), its thickness (t), its diameter (D), and the change in temperature across it (ΔT)

$$\text{thermal wedge} = \frac{\text{CTE} \times t \times \Delta T}{D}. \tag{15}$$

Given the combined effect of this thermal and the actual wedges, the errors for tilt and centration described in Sec. 3.6 can be re-calculated using the new index of refraction

$$n' = n_0 + \frac{\mathrm{d}n}{\mathrm{d}T}\Delta T, \tag{16}$$

where n_0 is the original index of refraction, $\mathrm{d}n/\mathrm{d}T$ is the change in index of the substrate material with temperature, and ΔT is the temperature change.

3.10 *Summary of Errors*

A summary of the expected alignment errors are listed in Table 1. "Eq. (#)" refers the equation used to calculate the error, and "Meas" indicates that the error is specific to the system hardware and must be estimated by the user. The errors are categorized as random or correlated, where random errors change between each measurement and correlated errors are consistent between measurements or couple into other errors. The total tilt and centration errors for each CGH are calculated by combining the values in the appropriate columns. Random errors are combined in quadrature and correlated errors by addition.

The dominate error sources depend on the specific system. For an autocollimator with 1 μrad resolution, the tilt uncertainty is about 0.5 μrad for each CGH. For a focal plane with 1 μm resolution (assuming no magnification in the focal plane and CGHB, $m = -0.5$), the centration uncertainty is about 0.66 μm for CGHB. In addition, when the substrate wedges are 2 μrad each, the resulting tilt and

Table 1 Summary of contributions to alignment error.

Sources of error	CGHA tilt	CGHA centration	CGHB tilt	CGHB centration	Random/correlated
Autocollimator calibration	Eq. (4)	—	Eq. (4)	OR Eq. (5)	C
Autocollimator beam wavefront	Eqs. (6)–(8)	Eqs. (6), (7), and (9)	Eqs. (6)–(8)	—	C
Spot centroiding	Meas	—	Meas	Meas	R
Hardware resolution	Meas	—	Meas	Meas	R
Kinematic mount repeatability	—	—	—	Meas/Eq. (1)	R
CGH wedge	—	—	Eqs. (10) and (11)	Eq. (12)	C
CGH writing error	Meas	Meas	Meas	Meas	C
Atmospheric effect	Eq. (14)	Eq. (13)	Eq. (14)	Eq. (13)	C
Temperature effect	—	—	Eqs. (10), (11), (15), and (16)	Eqs. (12), (15), and (16)	C

centration errors for CGHB are 1.85 μrad and 0.22 μm, respectively (assumes relative wedge orientation of 45 deg).

4 Two CGH Experiment

A system with two CGHs was aligned multiple times to estimate the alignment uncertainty for this procedure.[11] The system layout is shown in Fig. 14.

4.1 *Alignment Check*

The residual alignment error was measured with an independent optical test. In the region outside the FZPs, two extra patterns on each CGH act like two sets of spherical mirrors with a sphere on CGHA having a common "center of curvature" with a sphere on CGHB. When a point source is placed at the center of curvature for one set of mirrors, the displacement between the reflected spots shows the CGH misalignment, as in Fig. 15. Two sets of mirrors are needed to calculate the tilt and centration misalignments of CGHB to CGHA in both the x- and y-directions.

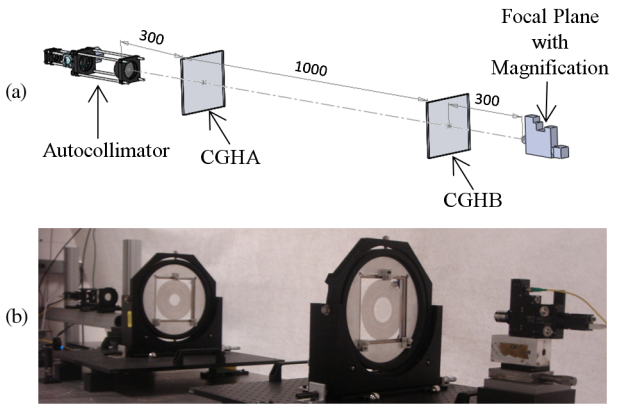

Fig. 14 (a) The optical system consists of two CGHs spaced 1 m apart with the autocollimator and focal plane on either end (distances in millimeters). (b) The experimental setup is pictured.

The tilt (α) and centration (Δ) misalignments of CGHB with respect to CGHA are calculated using the following set of equations:

$$\alpha = \frac{\sqrt{(\delta_{1x} - \delta_{2x})^2 + (\delta_{1y} - \delta_{2y})^2}}{2(L_1 + L_2)}$$
$$\Delta = \frac{\sqrt{(\delta_{1x}L_2 + \delta_{2x}L_1)^2 + (\delta_{1y}L_2 + \delta_{2y}L_1)^2}}{2(L_1 + L_2)}, \quad (17)$$

where δ_{1x} and δ_{1y} give the separation of the reflected spots in configuration Fig. 15(a), δ_{2x} and δ_{2y} give the separation of the reflected spots in configuration Fig. 15(b), and L_1 and L_2 are the distances between the point source and CGHB in each configuration, respectively. The signs of the separations are in the global coordinates. For small angles and decenters, the effect of plane parallel substrates is negligible.

4.2 *Results*

Table 2 shows the residual misalignment of CGHB with respect to CGHA using the spherical mirror check for 12 different alignments.

Some of the residual misalignment is error in the check itself. The misalignments are calculated based on the distance between spot centroids and uncertainty in their locations leads to uncertainty in the check. The magnitude of the centroid uncertainty, primarily due to the size/quality of the spots and wedge in the CGHs, must be estimated for the hardware, and Eq. (17) relates that uncertainty to the check uncertainty.

The expected errors are shown in Table 3. Based on experience with the setup, the writing error, atmospheric effects, and thermal effects are neglected.

The total uncertainty is calculated by combining the random errors in quadrature, which vary between alignments. For this experiment, the autocollimator was calibrated before each measurement, so we include that contribution in the

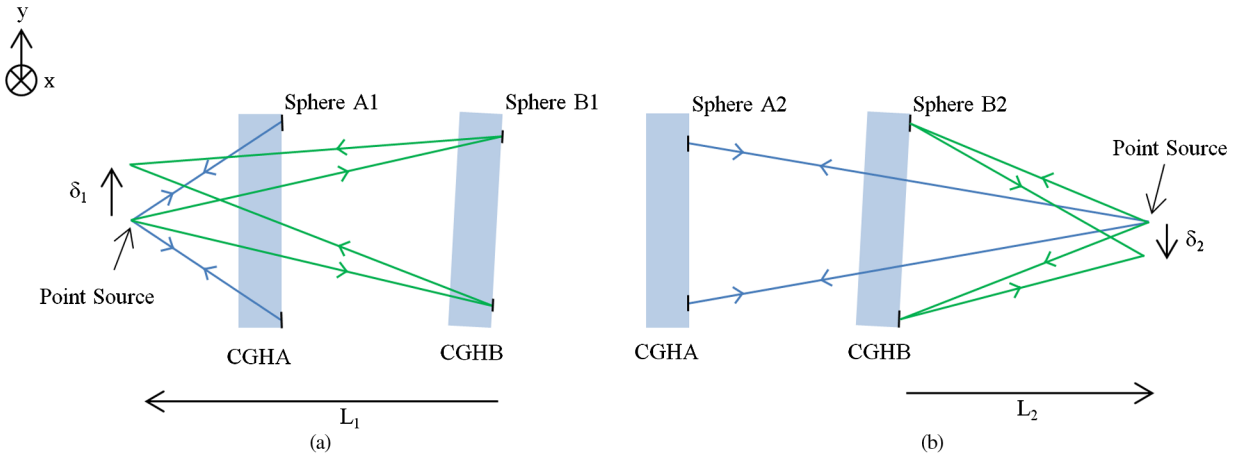

Fig. 15 The sphere check measures the residual error in the alignment procedure. (a) A point source is placed at the "center of curvature" of two spherical mirror patterns. The displacement between the reflected spots is measured to determine the misalignment of CGHB with respect to CGHA. (b) A second set of spherical mirror patterns is used with the point source placed on the opposite side of the substrates. The separation in the figure is not to scale.

Table 2 Statistics for spherical mirror alignment check.

Degree of freedom	Average	Standard deviation (1σ)
Tilt X	0.71 μrad	2.5 μrad
Tilt Y	0.76 μrad	1.34 μrad
Centration X	−0.32 μm	1.25 μm
Centration Y	−0.23 μm	0.64 μm
Tilt magnitude	1.04 μrad	2.83 μrad
Centration magnitude	0.39 μm	1.40 μm

random error as well. This test measures the angle of CGHB with respect to CGHA, so it cannot measure the tilt error from aberrations in the autocollimator beam wave front, which is equal for both substrates and is left out of the calculation. However, the CGHA centration error from the aberrated wave front will add bias, since it is the same for all alignments. The CGH wedge magnitude and orientation does not vary between alignments, which also add bias. Assuming that the error from the alignment check is small, the total expected and measured uncertainties are consistent, as shown in Table 4.

Table 4 Summary of expected and measured errors for two CGH systems.

	Tilt error (μrad)	Centration error (μm)
Expected (from analysis)	0.13 ± 3.06 1σ	0.09 ± 1.31 1σ
Measured (from experiment)	1.04 ± 2.83 1σ	0.39 ± 1.40 1σ

5 Conclusion

A procedure to align CGHs spaced meters apart in tilt and centration with low uncertainty was presented. This procedure described the alignment of CGH references only, but if the CGHs were well aligned to the optics individually,

Table 3 Summary of contributions to alignment error for two computer-generated hologram (CGH) systems.

Sources of error	CGHA tilt μrad (1σ)	CGHA centration μm (1σ)	CGHB tilt μrad (1σ)	CGHB centration μm (1σ)	Random/correlated
Autocollimator calibration	0	0	0	0.34	R
Autocollimator beam wavefront	0.64	0.08	0.64	0	C
Spot centroiding	1.77	0	1.77	0.2	R
Hardware resolution	1.25	0	1.25	0.14	R
Kinematic mount repeatability	0	0	0	1.25	R
CGH wedge	0	0	0.13	0.05	C

the optical system will also be accurately aligned. The use of CGHs as the external references provided several convenient advantages including the ability to write multiple patterns to a single substrate. The concept uses zero-order reflections to align the CGHs in tilt and first-order imaging to align them in centration. The same beam created the datum for tilt and centration giving lower uncertainties than the use of two separate beams. The process for aligning the references in tilt and centration was decoupled, which along with real-time feedback from the instruments makes the alignment straightforward and efficient.

The major sources of error were identified and equations were given for their contributions to the final uncertainty. Errors were classified as misalignments of CGHA and/or CGHB, as well as whether they were random or correlated. Since CGHA is used to align all CGHBs, it is worth making sure that it is a high-quality substrate with low wedge.

A system of two CGHs spaced 1 m apart was built to verify the analysis. Multiple alignments were performed, and an independent optical test quantified the alignment uncertainty. The procedure achieved a tilt uncertainty of 2.8 μrad 1σ and a centration uncertainty of 1.4 μm 1σ, which was consistent with the analysis. The tilt uncertainty was dominated by spot centroiding and hardware resolution, while the centration uncertainty was primarily due to the autocollimator calibration and the repeatability of the kinematic mounts.

The power of this procedure is that it does not rely on the surfaces of the optical system or any specific geometry. As long as the positions of the CGHs with respect to the optics are known, the geometry can be chosen to fit within the available space and maximize the sensitivity to misalignments. Once the tooling for the specific geometry is created, the procedure can be easily repeated allowing for efficient alignment of optical systems produced in high volume. Overall, this is a highly flexible, very low uncertainty alignment procedure that can be applied to a wide variety of optical systems. In fact, it is well suited for the alignment of any rotationally symmetric system that can accommodate the mounting of CGHs along its axis.

Acknowledgments

This work has been supported by HETDEX for use in the alignment of the new Wide Field Corrector. HETDEX is run by the University of Texas at Austin McDonald Observatory and Department of Astronomy with participation from the Ludwig-Maximilians-Universität München, Max-Planck-Institut für Extraterrestriche-Physik (MPE), Leibniz-Institut für Astrophysik Potsdam (AIP), Texas A&M University, Pennsylvania State University, Institut für Astrophysik Göttingen, University of Oxford, and Max-Planck-Institut für Astrophysik (MPA). In addition to Institutional support, HETDEX is funded by the National Science Foundation (Grant AST-0926815), by the State of Texas, by the US Air Force (AFRL FA9451-04-2-0355), by the Texas Norman Hackerman Advanced Research Program under Grants 003658-0005-2006 and 003658-0295-2007, and by generous support from private individuals and foundations.

References

1. Tesa Micro-Hite 3d CMM - Product Specifications, www.microhite3dcmm.com (accessed on 7 November).
2. J. H. Burge et al., "Use of a commercial laser tracker for optical alignment," *Proc. SPIE* **6676**, 66760E (2007).
3. Faro Laser Tracker, http://www2.faro.com/FaroIP/Files/File/Techsheets%20Download/04REF101-007%20-%20LTX%20-%20SEA_web.pdf (accessed on 7 November).
4. "Optical Alignment," Taylor Hobson Limited, pp. 10–18, Centaprint Limited, England (1998).
5. J. H. McLeod, "Axicons and their uses," *J. Opt. Soc. Am.* **50**(2), 166–166 (1960).
6. Z. Xinbao, Z. Bin, and L. Zhu, "Study of the tolerance of the non-diffracting beam to laser beam deflection," *J. Opt. A Pure Appl. Opt.* **4**(1), 78–83 (2002).
7. L. E. Coyle, M. B. Dubin, and J. H. Burge, "Characterization of an alignment procedure using an air bearing and off-the-shelf optics," *Proc. SPIE* **7793**, 77930C (2010).
8. R. Zehnder, J. H. Burge, and C. Zhao, "Use of computer-generated holograms for alignment of complex null correctors," *Proc. SPIE* **6273**, 62732S (2006).
9. J. H. Burge, R. Zehnder, and C. Zhao, "Optical alignment with computer-generated holograms," *Proc. SPIE* **6676**, 66760C (2007).
10. J. H. Burge, "An easy way to relate optical element motion to system pointing stability," *Proc. SPIE* **6288**, 62880I (2006).
11. L. E. Coyle, M. Dubin, and J. H. Burge, "Low uncertainty alignment procedure using computer generated holograms," *Proc. SPIE* **8131**, 81310B (2011).
12. Measurement report for fabricated CGH using Leica LMS IPRO (September 2012).
13. J. H. Churnside and R. J. Lataitis, "Wander of an optical beam in the turbulent atmosphere," *Appl. Opt.* **29**(7), 926–930 (1990).

Laura E. Coyle received a BA degree in physics from Colgate University in 2009 and an MS degree in optical sciences from the University of Arizona in 2011. She is currently pursuing a PhD in Dr. Burge's Large Optics Fabrication and Testing Group, where her interests include optical design, alignment, metrology, and systems engineering.

Matthew B. Dubin received a BSE in biomedical engineering from Duke University in 1993 and MS and PhD degrees in optical sciences in 1996 and 2002 from the University of Arizona. He is an associate research professor at the University of Arizona, where his interests include optical systems, metrology, alignment, and teaching.

James H. Burge received a BS in engineering physics from Ohio State University in 1987 and MS and PhD degrees in optical sciences in 1991 and 1993 from the University of Arizona. He is a professor at the University of Arizona with joint appointments in optical sciences and astronomy, where his interests are astronomical optics, optical fabrication and testing, optomechanics, and optical system engineering.